Thermal effects and space-charge limited transition in crossed-field devices

Samuel Marini, Felipe B. Rizzato, and Renato Pakter

Citation: Physics of Plasmas (1994-present) **21**, 083111 (2014); doi: 10.1063/1.4893313
View online: http://dx.doi.org/10.1063/1.4893313
View Table of Contents: http://scitation.aip.org/content/aip/journal/pop/21/8?ver=pdfcov
Published by the AIP Publishing

Thermal effects and space-charge limited transition in crossed-field devices

Samuel Marini, Felipe B. Rizzato, and Renato Pakter
Instituto de Física, Universidade Federal do Rio Grande do Sul, Caixa Postal 15051, 91501-970 Porto Alegre, RS, Brazil

(Received 12 June 2014; accepted 4 August 2014; published online 14 August 2014)

A fully kinetic model for the electron flow in a crossed field device is derived and used to determine the system stationary states. It is found that for low injection temperatures, there is a simultaneous presence of distinct stationary solutions and an abrupt transition between accelerating and space-charge limited regimes. On the other hand, for high injection temperatures, there is only a single stationary solution branch and the change between the regimes becomes continuous. For intermediate temperatures, it is then identified a critical point that separates the abrupt and continuous behaviors. It is also investigated how intrinsic space-charge oscillations may drive stationary states unstable in certain parameter regimes. The results are verified with N-particle self-consistent simulations. © *2014 AIP Publishing LLC*. [http://dx.doi.org/10.1063/1.4893313]

I. INTRODUCTION

Fully kinetic descriptions of long-range self-interacting systems are generally very difficult to obtain because these systems do not relax to the Maxwell-Boltzmann distribution and the tools of equilibrium statistical mechanics cannot be employed.[1] This is the case of electron flows in the presence of crossed electric and magnetic fields which are fundamental for the development of several advanced applications in areas ranging from microwave sources[2] to space propulsion,[3] as well as in the semiconductor industry.[4] The study of the electron dynamics in such field configuration was pioneered by Hull,[5] who showed that a magnetic field may limit the particle flow from the cathode to the anode. This result was based on a single-particle model that assumes given external electromagnetic fields. More recently, a large number of papers have investigated the equilibrium and stability of these systems by explicitly taking into account the particles self-fields.[6–15] The self-fields may play a major role in the dynamics since they can also limit the particles flow from the cathode to the anode as the current density exceeds a certain threshold and a space-charge limited (SCL) regime emerges.[6,10,16] However, given the afore mentioned complexity that long ranged self-fields add to the problem, the large majority of the theoretical analysis done so far are based on models that assume that the electron flow is either completely cold or is a fluid with an *a priori* postulated equation of state. In contrast to a kinetic description, these models may not properly take into account the thermal effects.

In this paper, we derive a fully kinetic model for the electron flow in a crossed field device. In particular, we consider a nonrelativistic planar gap device.[8,10,11,13,14] In the thermodynamic limit, where the number of particles goes to infinity while the total mass and charge are fixed, the electron flow is described by the Vlasov equation.[17,18] A theory is then developed to determine the stationary states of the corresponding Vlasov-Poisson system. We find that for relatively low injection temperatures, the system exhibits multiple stationary solutions as one approaches the limiting current, indicating the occurrence of a nonequilibrium first order phase transition.[19,20] On the other hand, for high injection temperatures, there is only a single stationary solution branch and the conversion to the SCL regime is continuous. For intermediate temperatures, we then identify a critical point that separates the abrupt and the continuous behavior. We also find that for vanishing small injection velocities, some of the stationary solutions become unstable due to space-charge oscillations. In this case, the system is driven to a different stationary state which is also predicted by the theory.

The paper is organized as follows. In Sec. II, we introduce the model for the nonrelativistic planar crossed-field gap and write the Vlasov-Poisson system that describes its kinetic evolution. In Sec. III, we develop the theory to determine the stationary states for the kinetic equations. Special attention is given to the transition between accelerating and SCL regimes. We also present results from N-particle self-consistent simulations that confirm the theoretical findings. In Sec. IV, we investigate the particular case where the injected electron beam presents particles with vanishing small velocities. In this case, we find that the stationary solution described in Sec. III becomes unstable and the system is driven to a different stationary state which can also be predicted by the theory. In Sec. V, we conclude the paper.

II. MODEL

A schematic diagram and field configuration of a nonrelativistic planar crossed-field gap is presented in Fig. 1. The cathode at $y = 0$ is kept at zero electrical potential, and the

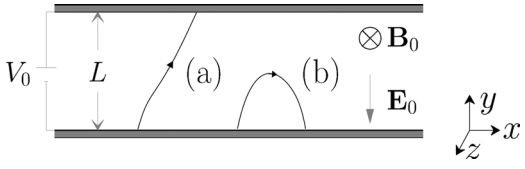

FIG. 1. A schematic diagram of a nonrelativistic planar crossed-field gap. The curves correspond to the trajectories of test electrons emitted from the cathode with zero velocity in the case (a) $V_0 > V_H$ and (b) $V_0 < V_H$.

anode at $y=L$ is held at a potential V_0, generating a uniform electric field $\mathbf{E}_0 = -(V_0/L)\hat{\mathbf{y}}$ in the gap region $0<y<L$. In this region, there is also an applied uniform constant magnetic field $\mathbf{B}_0 = -B_0\hat{\mathbf{z}}$. Examples of trajectories of test electrons that enter in the gap region with vanishing velocities are also shown in Fig. 1. The electrons are accelerated along the y direction by $\mathbf{E}_0$ and deflected clockwise by $\mathbf{B}_0$. If the accelerating potential satisfies $V_0 > V_H$, where $V_H = eB_0^2L^2/2m$ is the Hull potential, m and $-e$ are mass and charge of the electron, then the electron gains enough energy to reach the anode [trajectory (a)]. On the other hand, if $V_0 < V_H$ then the magnetic field force is strong enough to push the electron back to the cathode [trajectory (b)]. Once an electron reaches the cathode or the anode, it is absorbed and leaves the system.

Due to the system symmetry, during operation, the cathode is assumed to emit not single electrons but infinite charge sheets parallel to the x–z plane. Hence, the one particle distribution function in phase space $f(\mathbf{r}, \mathbf{p}, t)$ will only depend on the y spatial coordinate. Its evolution is dictated by the Vlasov equation[18]

$$\frac{df}{dt} = \frac{\partial f}{\partial t} + \frac{\partial H}{\partial p_y}\frac{\partial f}{\partial y} - \frac{\partial H}{\partial y}\frac{\partial f}{\partial p_y} = 0, \tag{1}$$

where $H = (\mathbf{p}+e\mathbf{A})^2/2m - e\phi$ is the single particle Hamiltonian and $\mathbf{A}$ and ϕ are the vector and scalar electromagnetic potentials. The scalar potential is self-consistently determined from the particle distribution by the Poisson equation

$$\frac{\partial^2\phi}{\partial y^2} = \frac{e}{\epsilon_0}\, n(y), \tag{2}$$

satisfying the boundary conditions $\phi(0)=0$ and $\phi(L)=V_0$, where $n(y) = \int f(y,\mathbf{p})\, d\mathbf{p}$ is the electron density. The background magnetic field is derivable from a vector potential $\mathbf{A}_0 = -B_0 y\hat{\mathbf{x}}$, such that $\mathbf{B}_0 = \nabla\times\mathbf{A}_0$. It is clear that the electrons generate current densities with both x and y components (see Fig. 1). These currents create a self-magnetic field that tend to screen B_0. Nevertheless, if we assume that the gap region is sufficiently thin, we can safely neglect the self-magnetic fields[13] and take $\mathbf{A}=\mathbf{A}_0$. The single particle Hamiltonian is then given by

$$H = \frac{1}{2m}\left[(p_x + eB_0 y)^2 + p_y^2 + p_z^2\right] - e\phi(y). \tag{3}$$

Because the Hamiltonian does not depend on x and z, the canonical momentum components p_x and p_z are constants of motion. Their values are determined by the electron velocity when entering the gap region. For simplicity, we assume that the electrons are injected with velocities normal to the cathode, such that $p_x = p_z = 0$. Note that this condition does not imply that the velocity parallel to the cathode is always zero. In fact, because velocity and canonical momentum are related by $=(\mathbf{p}+e\mathbf{A})/m$, the particles are accelerated in the x direction, such that $v_x = eB_0 y/m$. Finally, it is worth noting that because the convective derivative of $f(y, p_y, t)$ vanishes according to the Vlasov equation (1), the system evolves over the phase space as an incompressible fluid.

III. STATIONARY STATES AND TRANSITION TO SPACE-CHARGE LIMITED REGIME

As the device is *turned on* and electrons start to flow in the gap region, the system is expected to reach a stationary state after some transient time. Our aim is to determine this stationary state and, particularly, if it is in the accelerating regime or in the SCL regime—when the self-fields are large enough to screen the accelerating field at the cathode. Let us consider that the electrons are injected from the cathode according to a given velocity distribution. Namely, a waterbag satisfying

$$f(y=0,p_y) = \frac{n_0}{p_{0max}-p_{0min}}, \tag{4}$$

for $p_{0min} \le p_y \le p_{0max}$ and zero elsewhere, where n_0 is the particles density at the cathode. The parameters n_0, p_{0min}, and p_{0max} completely determine the injected beam. The technique employed here can be readily generalized to other velocity distributions by approximating them by a series of waterbags.[21] Once the stationary state has been achieved, all the quantities become time independent, in particular the single electron Hamiltonian (3). It is thus straightforward to write the momentum of a given electron as

$$p_y(p_0,y) = \pm[p_0^2 + 2em\phi(y) - e^2B_0^2y^2]^{1/2}, \tag{5}$$

where p_0 is its momentum at the cathode and the plus (minus) sign refers to an electron that is moving towards the anode (cathode). All the particles are distributed in the phase space region between the least and most energetic trajectories $p_y(p_{0min}, y)$ and $p_y(p_{0max}, y)$. Moreover, because the Vlasov equation (1) imposes that the electron flow is incompressible in the phase space, the distribution everywhere inside this region has the same density as that of $y=0$, namely $n_0/(p_{0max}-p_{0min})$. We concentrate on magnetic insulated cases where $V_0 < V_H - p_{0max}^2/2me$, and all the particles ejected from the cathode eventually return to it. Taking all these points into consideration, we can finally write the density of particles as

$$n(y) = 2n_0\frac{|p_y(p_{0max},y)| - |p_y(p_{0min},y)|}{p_{0max}-p_{0min}}, \tag{6}$$

where the factor "2" accounts for the fact that there is an equal number of particles moving to and from the cathode and $p_y(p_{0max}, y)$ and $p_y(p_{0min}, y)$ are real functions to be considered zero whenever they become imaginary. Substituting this in Eq. (2), we obtain a closed equation for the electric potential $\phi(y)$ in the stationary state.

It is convenient to define dimensionless parameters $\nu_0 = V_0/V_H$, $\eta_0 = en_0L^2/\epsilon_0V_0$, $\bar{p}_0 = (p_{0min}+p_{0max})/2eB_0L$, and $T_0 = (p_{0max}-p_{0min})^2/12e^2B_0^2L^2$ which measure, respectively, the normalized accelerating potential and the electron density, the average momentum, and the temperature (momentum spread) at injection. To determine if a certain stationary solution is accelerating or SCL, we compute the electric field at the cathode $E_c = -\partial\phi/\partial y|_{y=0}$. In Fig. 2, we plot E_c as a function of the normalized electron density for $\nu_0 = 0.8$, $\bar{p}_0 = 0.2$, and $T_0 = 8.3\times10^{-4}$. When $\eta_0 \to 0$, the

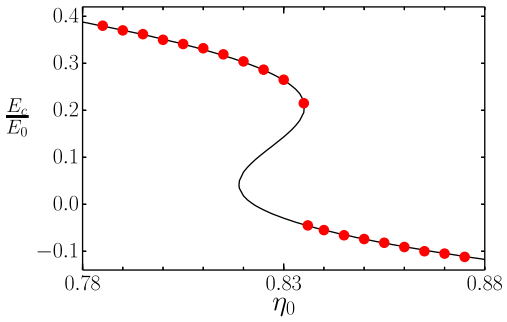

FIG. 2. Normalized electric field at the cathode for the stationary state as a function of the normalized electron density η_0 for $T_0 = 8.3 \times 10^{-4}$, $\nu_0 = 0.8$, and $\bar{p}_0 = 0.2$. The solid line corresponds to results from the theory, whereas the symbols—results from the simulation. As a consequence of the existence of multiple stationary solutions, the system suffers an abrupt transition from the accelerating ($E_c/E_0 > 0$) to the SCL ($E_c/E_0 < 0$) regime.

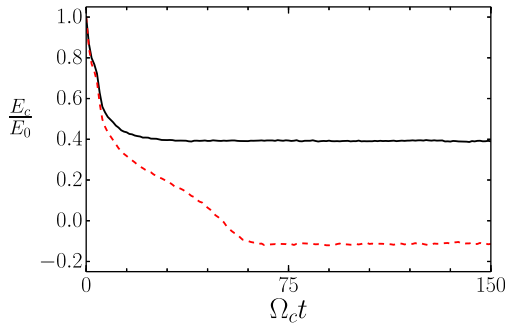

FIG. 3. Time evolution of the normalized electric field at the cathode for two simulation runs with the same parameters as in Fig. 2 and two different normalized electron densities: $\eta_0 = 0.78$ (black solid curve) and $\eta_0 = 0.88$ (red dashed curve). After a transient time, the cathode field saturates as the system reaches the stationary state. For $\eta_0 = 0.78$, the stationary state corresponds to an accelerating regime with $E_c/E_0 > 0$ for large t, whereas for $\eta_0 = 0.88$, it corresponds to a SCL regime with $E_c/E_0 < 0$ after saturation.

electron density is so small that the normalized potential approaches the vacuum solution of Eq. (2), $\phi(y) = V_0 y/L$, and $E_c \approx E_0 \equiv -V_0/L$. As η_0 increases, E_c/E_0 decreases because progressively more charge is present in the gap region, depleting the accelerating electric field. On the other hand, for large values of the normalized electron density, above $\eta_0 \approx 0.84$, the amount of charge in the gap becomes large enough to completely screen the accelerating field and a single stationary solution that corresponds to SCL states with $E_c/E_0 < 0$ is found. In the intermediate region $0.820 < \eta_0 < 0.835$, we find the presence of three different stationary solutions, indicating that the system may *jump* from one solution branch to the other with a small variation of η_0. Because the system is not in thermodynamic equilibrium—it evolves according to Vlasov equation instead of Boltzmann equation—such a jump corresponds to a nonequilibrium first order phase transition[19,20] between accelerating and SCL regimes.

To verify this scenario, we run N-particle self-consistent simulations. In the simulations, charge sheets are injected from the cathode according to Eq. (4). The dynamics of the ith sheet inside the gap region is derived from the Hamiltonian (3) as $\ddot{y}_i = -\Omega_c^2 y_i - e(E_0 + E_s^i)/m$, where the dots stand for time derivatives, $\Omega_c = eB_0/m$ is the cyclotron frequency, and E_s^i is the self electric-field acting upon the ith sheet due to the interaction with the remainder charges in the systems, which can be readily obtained using Green's functions.[22] To model the charging process in real devices, we initialize the simulation with an empty gap region and compute the electric field at the cathode $E_c(t)$ as the charge builds up in the system. In Fig. 3, we present the time evolution of the cathode field obtained from the simulation for two values of η_0. In both cases, $E_c(t)/E_0$ starts at unity, corresponding to an empty gap, and quickly drops as charge starts to flow into the system. After some transient time, $E_c(t)$ saturates, indicating that the system has reached a stationary state. Note that while for the lower normalized density case $\eta_0 = 0.78$, the stationary regime is characterized by an accelerating cathode field with a saturated value $E_c(t)/E_0 > 0$, for the higher density $\eta_0 = 0.88$, the system becomes SCL in the stationary regime with a saturated value $E_c(t)/E_0 < 0$, in agreement with the theoretical results of Fig. 2.

In order to investigate the stationary state attained by the system for different normalized electron densities, we performed a series of N-particle simulations for different η_0 and computed the saturated values of the cathode electric field. The results are shown by the symbols in Fig. 2. We see a very good agreement with the results predicted by the theory. In particular, in the region with multiple solutions, the system follows the upper (accelerating) branch of the theoretically predicted stationary solutions. At $\eta_0 = 0.836$, this branch ceases and the system jumps from the accelerating ($E_c/E_0 = 0.2$) to the SCL regime ($E_c/E_0 = -0.05$), characterizing the first-order phase transition. In Fig. 4, we compare the stationary distribution of charge sheets in phase-space obtained from the simulation right before and after the transition. We also present in the figure, the theoretical $p_y(p_{0min}, y)$ and $p_y(p_{0max}, y)$ curves to show that they agree very well with the boundaries of the particles distribution from the simulation. While in panel (a) for $\eta_0 = 0.835$ the charge distribution is nearly semiannular, for the slightly higher value $\eta_0 = 0.836$ of panel (b), it becomes much thicker in the center of the gap ($y \approx 0.5$), occupying most of the empty inner region of Fig. 4(a). This leads to an increase of the total charge in the gap of 22% which is responsible for the onset of the SCL regime. In the simulations, we observe that as

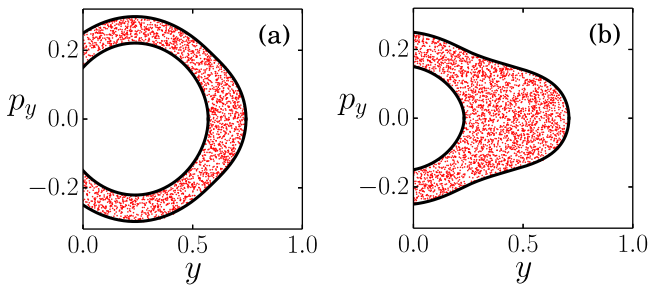

FIG. 4. Snapshots of the phase space obtained from the simulation after the stationary state has been attained. The parameters correspond to those of Fig. 2 in the vicinity of the abrupt transition. A slight change in the normalized electron density from (a) $\eta_0 = 0.835$ to (b) $\eta_0 = 0.836$ drives the system from the accelerating to the SCL regime, producing a dramatic change in the charge distribution. Thick solid lines correspond to the charge distribution boundaries predicted by the theory. Position and momentum are normalized to L and qB_0L, respectively.

soon as the electrons start to be injected in the initially empty gap, they always tend to form a semiannular distribution similar to that of Fig. 4(a), regardless of the value of η_0. This corresponds to the quick drop of E_c/E_0 seen in Fig. 3 up to $\Omega_c t \approx 10$ for both cases presented. If η_0 is below the phase transition value (black solid curve in Fig. 3), this distribution is very close to a stationary state of the system and E_c/E_0 soon saturates. On the other hand, if η_0 is above the phase transition value (red dashed line in Fig. 3), the semiannular distribution does not correspond to a stationary solution anymore and the charge continues to *slowly* build up in the gap until the SCL stationary regime is finally reached.

Let us consider a case with a larger injection temperature. In Fig. 5, we plot the stationary cathode electric field as a function of η_0 for $T_0 = 3.3 \times 10^{-3}$. In contrast to the case of Fig. 2, now the theory (solid line) predicts a single stationary solution branch and consequently, a continuous change from accelerating to SCL regime as the $E_c = 0$ axis is crossed. This is confirmed by the N-particle simulations (symbols). This suggests the existence of a critical injection temperature T_{0c} which separates the continuous and the abrupt behavior. To verify this, we construct a phase-diagram η_0 vs. T_0, determining for which parameters we find multiple stationary solutions and for which the change is continuous. The results are shown in Fig. 6 where a critical injection temperature $T_{0c} \approx 1.4 \times 10^{-3}$ is found. For temperatures above T_{0c}, the dashed line corresponds to the points where $E_c = 0$ and the system is switching continuously from the accelerating to the SCL stationary regime. Below T_{0c}, the region between the dotted and the solid line corresponds to parameter values for which multiple stationary solutions are found. In this case, the system suffers an abrupt transition to the SCL regime as it crosses the solid line.

IV. INSTABILITY FOR INJECTION WITH VANISHING SMALL VELOCITIES

When one considers the limit $p_{0min} \to 0$, another interesting dynamical feature emerges. This is illustrated in Fig. 7 where we present results for $p_{0min} = 0$, $\bar{p}_0 = 0.4$, $\nu_0 = 0.8$, and $\eta_0 = 0.6$. For this set of parameters, Eq. (2) with a density given by Eq. (6) predicts a single stationary solution with $E_c/E_0 = 0.645$, which is represented by the green dashed line in panel (a) and whose corresponding $p_y(p_{0min}, y)$ and $p_y(p_{0max}, y)$ curves are shown in panels (b) and (c). The solid line in panel (a) is $E_c(t)$ obtained from the simulation. We notice that $E_c(t)/E_0$ *quickly* drops from the unity and approaches the theoretical predicted value, where it reaches a sort of plateau, as expected. However, at longer times ($\Omega_c t \sim 10^3$), $E_c(t)/E_0$ starts to deviate, reaching a new plateau at $E_c(t)/E_0 \approx 0.37$.

To clarify what is happening, we show snapshots of the phase space obtained at different times in Figs. 7(b)–7(d). While for $\Omega_c t = 10^2$ (b) the borders of the N-particle distribution agree with the theory, for $\Omega_c t = 2 \times 10^3$ (c), some particles start to populate the region inside $p_y(p_{0min}, y)$. This occurs because the charges that enter in the system with vanishingly small momentum closely follow the $p_y(p_{0min}, y)$ curve in phase space. In the absence of any perturbation, they would return to the cathode and reach it with a correspondingly small momentum. However, because of

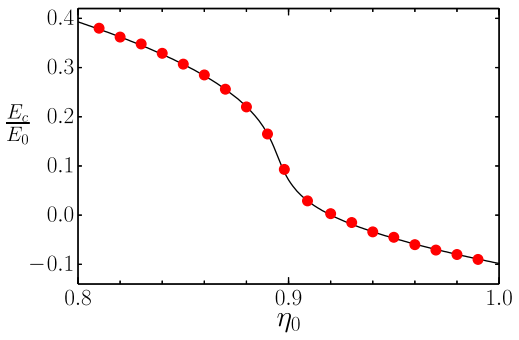

FIG. 5. Normalized electric field at the cathode for the stationary state as a function of the normalized electron density η_0 for $T_0 = 3.3 \times 10^{-3}$. The remainder parameters are the same as in Fig. 2. The theory (solid line) predicts a single stationary solution branch and a continuous change from accelerating to SCL regime, which is verified by the simulation (symbols).

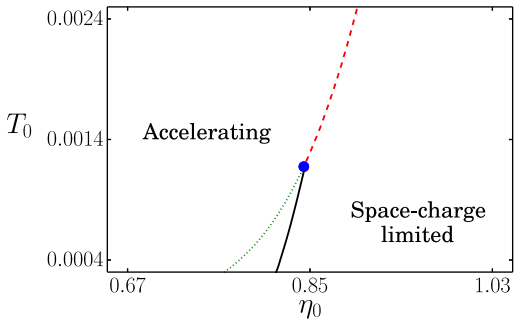

FIG. 6. Parameter space T_0 vs. η_0 showing where the conversion between accelerating and SCL regimes is continuous (dashed line) or abrupt (solid line), and the critical point (solid dot) that separates them. The region between the solid and the dotted line corresponds to the region of multiple stationary solutions.

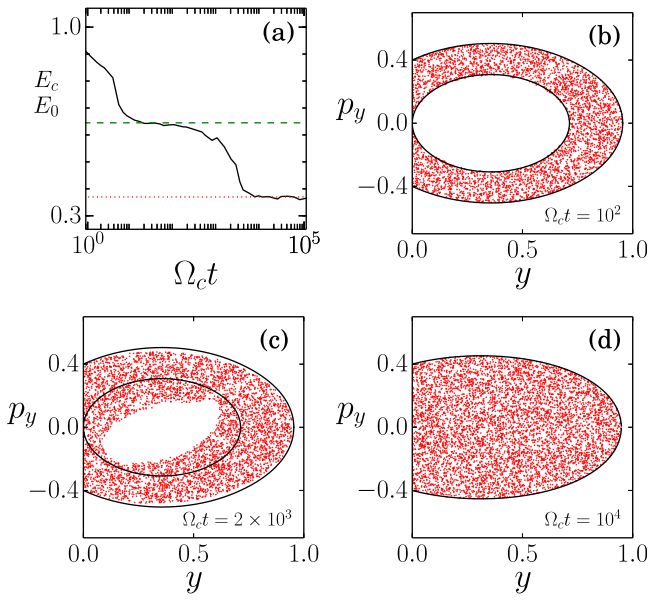

FIG. 7. Results for $p_{0min} = 0$. In (a), the time evolution for the cathode electric field. The lines are theoretically predicted values. In (b)–(d), the phase space at different times. Solid lines correspond to the charge distribution boundaries predicted by the theory. Position and momentum are normalized to L and qB_0L, respectively.

oscillations in the electron distribution, some of these sheets loose energy while traversing the system and are unable to reach back the cathode, becoming trapped inside the gap region. This process continues on and on, building progressively more charge in the system. It only ceases when the region inside $p_y(p_{0min}, y)$ is completely filled to the maximum density allowed by the Vlasov equation. Hence, for the *final* stationary state of Fig. 7(d), we can write the particles density as given by Eq. (6) with $p_y(p_{0min}, y) = 0$, i.e.,

$$n(y) = 2n_0 \frac{|p_y(p_{0max}, y)|}{p_{0max}}. \tag{7}$$

Substituting Eq. (7) in the Poisson equation (2), we then obtain a closed equation for the *final* stationary state attained by a system with vanishing small velocities. For the parameters of Fig. 7, this *final* stationary state is predicted to have $E_c(t)/E_0 = 0.371$ [red dotted line in Fig. 7(a)]. The corresponding theoretical $p_y(p_{0max}, y)$ curve is also shown in Fig. 7(d). Both results clearly agree with the simulation. This process that unstabilizes the stationary state of Fig. 7(b) is similar to the modulational instability discussed in Ref. 11 in the context of cold electron flows. The main difference is that there, the instability is driven by an external ac voltage added to V_0, whereas here, it is driven by intrinsic oscillations of the electron distribution.

V. CONCLUSION

To conclude, we have investigated a fully kinetic model for the electron flow in a crossed field device and developed a theory to determine its stationary states. We found that depending on the parameters of the system, it may present either a single or multiple stationary solutions as the limiting current is approached. While in the former case the conversion from accelerating to SCL regime is continuous, in the latter case, it is abrupt, characterizing a nonequilibrium first-order phase transition. It was then identified a critical point that separates the continuous and the abrupt behavior. We also found that some stationary states become unstable due to space-charge oscillations if there are particles injected with vanishing velocities. Results were verified with N-particle self-consistent simulations. The phase transitions discussed here add to the already known rich behavior in the parameter space of the planar crossed-field gap.[6,10] Given these rich properties, it is anticipated that this model may also be used as a test bed for the study of phase transitions in driven long-range interacting systems.

ACKNOWLEDGMENTS

This work was partially supported by CNPq and FAPERGS, Brazil, and by the US-AFOSR under Grant No. FA9550-12-1-0438. We thank Y. Levin for useful discussions.

[1]A. Campa, T. Dauxois, and S. Ruffo, Phys. Rep. **480**, 57 (2009); Y. Levin, R. Pakter, F. B. Rizzato, T. N. Teles, and F. P. da C. Benetti, Phys. Rep. **535**, 1 (2014).
[2]A. S. Gilmour, *Klystrons, Traveling Wave Tubes, Magnetrons, Crossed-Field Amplifiers, and Gyrotrons* (Artech House, Norwood, MA, 2011).
[3]D. M. Goebel and I. Katz, *Fundamentals of Electric Propulsion: Ion and Hall Thrusters* (John Wiley & Sons, Inc., Hoboken, NJ, 2008).
[4]C. Ye, H. He, F. Huang, Y. Liu, and X. Wang, Phys. Plasmas **21**, 043509 (2014).
[5]A. W. Hull, Phys. Rev. **18**, 31 (1921).
[6]M. A. Pollack, Ph.D. thesis, University of California, Berkeley, CA, 1962.
[7]J. Swegle and E. Ott, Phys. Rev. Lett. **46**, 929 (1981).
[8]R. C. Davidson and H. S. Uhm, Phys. Rev. A **32**, 3554 (1985).
[9]R. C. Davidson, H.-W. Chan, C. Chen, and S. Lund, Rev. Mod. Phys. **63**, 341 (1991).
[10]Y. Y. Lau, P. J. Christenson, and D. Chernin, Phys. Fluids B **5**, 4486 (1993).
[11]P. J. Christenson and Y. Y. Lau, Phys. Rev. Lett. **76**, 3324 (1996).
[12]D. J. Kaup, Phys. Plasmas **8**, 2473 (2001).
[13]G. H. Goedecke, B. T. Davis, C. Chen, and C. V. Baker, Phys. Plasmas **12**, 113104 (2005).
[14]G. H. Goedecke, B. T. Davis, and C. Chen, Phys. Plasmas **13**, 083104, (2006).
[15]Y. Y. Lau, J. W. Luginsland, K. L. Cartwright, D. H. Simon, W. Tang, B. W. Hoff, and R. M. Gilgenbach, Phys. Plasmas **17**, 033102 (2010).
[16]C. D. Child, Phys. Rev. **32**, 492 (1911); I. Langmuir, *ibid.* **21**, 419 (1923).
[17]W. Braun and K. Hepp, Commun. Math. Phys. **56**, 101 (1977).
[18]R. C. Davidson, *Physics of Nonneutral Plasmas* (Imperial College Press, London, 2001).
[19]R. Pakter and Y. Levin, Phys. Rev. Lett. **106**, 200603 (2011).
[20]A. Antoniazzi, D. Fanelli, S. Ruffo, and Y. Y. Yamaguchi, Phys. Rev. Lett. **99**, 040601 (2007).
[21]Y. Levin, R. Pakter, and T. N. Teles, Phys. Rev. Lett. **100**, 040604 (2008); T. N. Teles, R. Pakter, and Y. Levin, Appl. Phys. Lett. **95**, 173501 (2009).
[22]F. B. Rizzato, R. Pakter, and Y. Levin, Phys. Rev. E **80**, 021109 (2009).